Biophysical Journal, Volume 96

Supporting Material

Traction stresses and translational distortion of the nucleus during fibroblast migration on a physiologically relevant ECM mimic

Zhi Pan, Kaustabh Ghosh, Yajie Liu, Richard A. F. Clark, and Miriam H. Rafailovich

Orientation and Dynamics of Peptides in Membranes Calculated from ^{2}H-NMR Data

Erik Strandberg*, Santi Esteban-Martin[†], Jesús Salgado[†,‡], Anne S. Ulrich*[,§]

* Karlsruhe Institute of Technology, Institute for Biological Interfaces, Forschungszentrum Karlsruhe, P.O.B. 3640, 76021 Karlsruhe, Germany.
† Instituto de Ciencia Molecular, Universidad de Valencia, 46980 Paterna (Valencia), Spain.
‡ Departamento de Bioquímica y Biología Molecular, Universidad de Valencia, 46100 Burjassot (Valencia), Spain
§ Institute of Organic Chemistry, University of Karlsruhe, Fritz-Haber-Weg 6, 76131 Karlsruhe, Germany.

Supplementary Material

1. Definition of α-helical structure parameters relevant for the ^{2}H NMR analysis

2. Comments to experimental data

3. Evaluation of data fits

4. Detailed analysis of Model 5

5. Influence of S^i on the fits of Models 4, 5 and 6

1. Definition of α-helical structure parameters relevant for the ^{2}H NMR analysis

The angles and conventions used in the analysis are defined in **Figure S1**, using the same conventions as reported before for PGLa (1-5), and in a way similar to that described previous for WALP (in **Figure 1** of reference (6)).

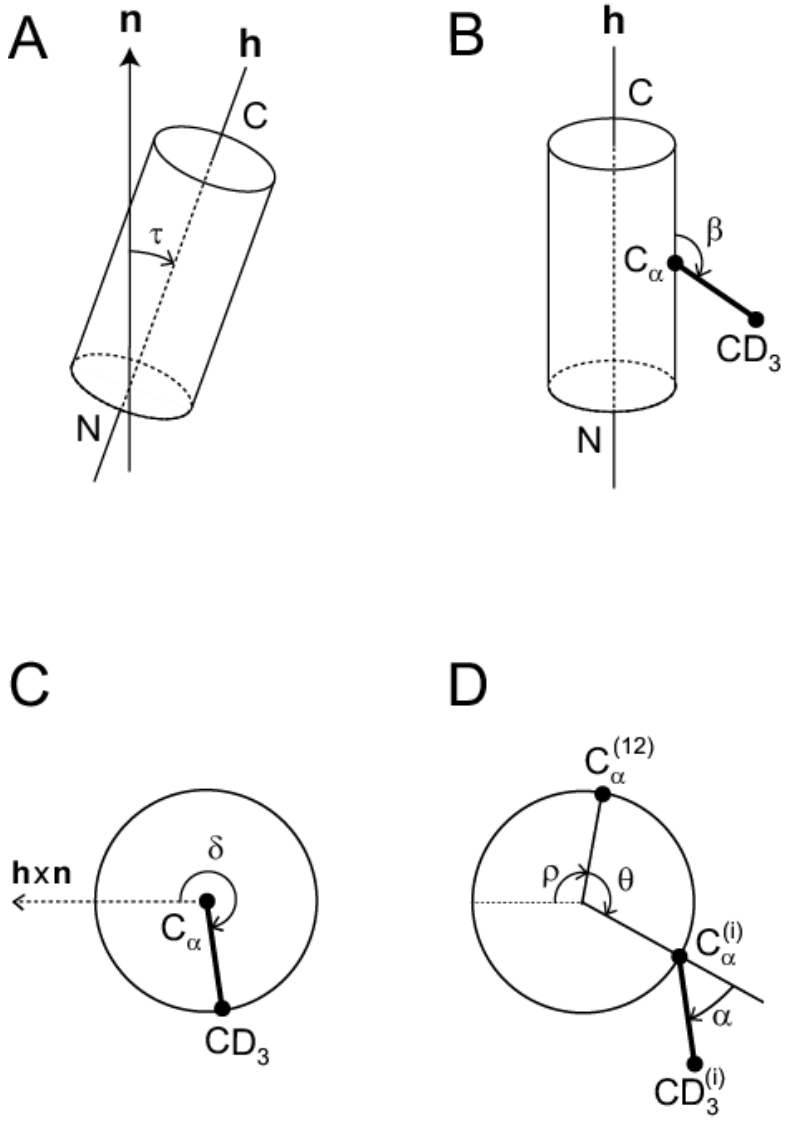

Figure S1. Definition of angles determining the orientation and geometry of the peptide used in this work. (A) The tilt angle, τ, is the angle between the helical axis **h** (going from the N-terminus to the C-terminus) and the bilayer normal, **n**. (B) The angle between the helix axis and the C_α–C_β bond is called β. (C) The orientation of the C_α–C_β bond around the helix axis is defined by the angle δ, which is the angle between the projection of the C_α–C_β bond onto a plane perpendicular to the helix axis, and a reference line, **h×n**, which is perpendicular to both the helix axis and the bilayer normal. (D) The angle δ is the sum of ρ, the azimuthal rotation angle, α, the angle between the C_α–C_β bond and a line from the center of the helix through the C_α, and θ, the angle around the helix between the C_α of the reference residue (position 12) and the C_α of the observed residue. The angle between two consecutive residues around the helix is called γ and for residue i, θ = (i-12)γ. α, β, and γ are structural parameters determining the helical structure of the peptide, and are assumed to be the same for all residues in the helix. τ and ρ are orientational angles determined from a fit of experimental data.

2. Comments to experimental data

Scaling of experimental data

When a peptide is rotating fast around the bilayer normal, the orientation-dependent quadrupolar splittings can be determined using unoriented NMR samples. In this case, the observed Pake splitting is related by a factor of -1/2 to the relevant splitting $\Delta\nu_q$ that would be observed in an oriented sample aligned with its normal parallel to the static magnetic field. To compare splittings from oriented and unoriented samples as they were published in the literature, all splittings from unoriented samples have been multiplied by 2 in this study. That way, the same $\Delta\nu_q^0$ value and S values between 0 and 1 can be used for all systems.

^{2}H-NMR splittings for PGLa/MAG2

For PGLa in 1:1 mixtures with magainin 2, quadrupolar splittings were measured for 8 positions labeled with Ala-d_3. Data from PGLa in which Gly-11 was replaced with Ala-d_3 did not fit with the rest of the data points and was excluded from the analysis. It should be noted that in the original paper (5) the splitting from position 10 was erroneously reported as 26.5 kHz; the correct value of 29.2 kHz was used in the calculations both in that paper and in the present study.

3. Evaluation of data fits

RMSD plots

The rmsd analysis to obtain the best-fit orientational angles can be visualized in two-dimensional τ/ρ-plots as illustrated in **Figure S2**. Here, each combination of the helix tilt and azimuthal rotation angles is mapped to its corresponding rmsd value as indicated by a gray scale. As an example we show the analysis of PGLa in the I-state (Model 2). Note that due to the symmetry within a lipid bilayer the error function is redundant, with $R(\tau, \rho) = R(\tau + 180^\circ, \rho) = R(180^\circ - \tau, \rho + 180^\circ)$. This means that it is not necessary to display the full range (0-360º) for both angles, but it is enough to show them in the range of 0-180º, or equivalently to display τ in the range of 0-90º and ρ in the range of 0-360º. To comply with the conventions used in previous publications of PGLa and WALP23, also in this study we will quote τ and ρ in the range of 0-180º for PGLa, and τ in the range of 0-90º and ρ in the range of 0-360º for WALP23.

Helical wave plots

Apart from using error plots as in **Figure S2**, it is also instructive to check the quality of the fits with a quadrupolar helical wave plot, as illustrated in **Figure S3**. This curve is calculated from the best-fit parameters (τ, ρ, *S*), and the experimental data points are plotted for each labeled side chain as a function of its angular position around the helix axis, as in a helical wheel representation. **Figure S3A** shows the quadrupolar wave of PGLa in the S-state, and **Figure S3B** shows the corresponding curve for WALP23 in DMPC, illustrating the striking difference between these curves arising from the respective peptide orientations. In both cases the fit is reasonably good for all data points, confirming that (i) the assumption of an ideal α-helical structure was an appropriate choice, and that (ii) none of the labels has introduced significant local structural perturbations.

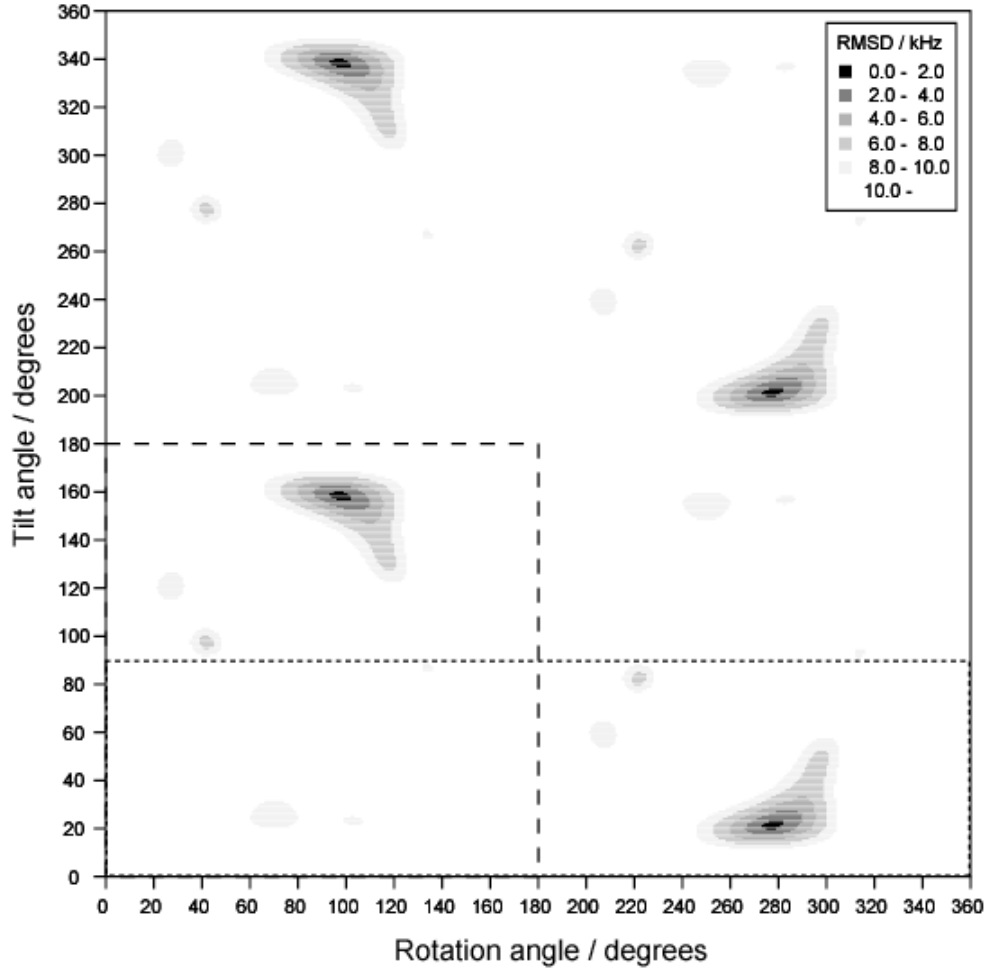

Figure S2. Plot of rmsd between calculated and experimental quadrupolar splittings, illustrated here for PGLa in the I-state, using the scaled static model with $\Delta\nu_q^0$ = 74 kHz (S^i=0.88). Darker areas have a smaller rmsd value. The τ/ρ-plot has a four-fold degeneracy, so that all possible orientations of the peptide are represented in either the dashed box (τ in the range 0-90º and ρ in the range 0-360º) or the dotted box (τ in the range 0-180º and ρ in the range 0-180º). The former ranges are used to represent PGLa orientations, while the latter ones are used for WALP23, in line with previous publications.

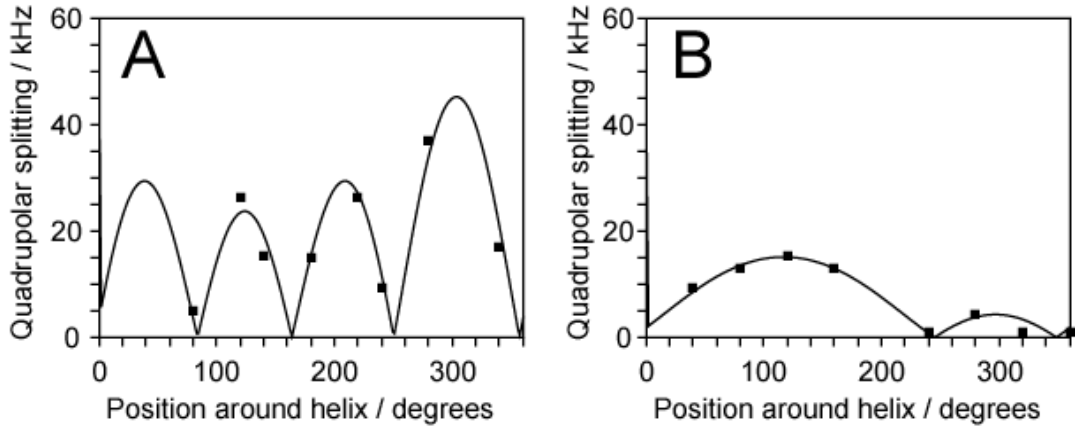

Figure S3. Helical wave plots fitted to the experimental ^{2}H-NMR quadrupolar splittings (filled squares) as a function of the Ala-d_3 angular position around the helix. The curve is calculated using Model 3 and the three best-fit parameters values (τ, ρ, *S*). (A) PGLa in the S-state, with best fit parameters of τ=98º, ρ=115º, and *S*=0.70. (B) WALP23 in DMPC, with best fit parameters τ=7º, ρ=302, and S=0.72. The other best-fit values are given in **Table 1** of the main text.

Influence of σ_ρ on the helical wave plots

The general averaging effect due to Gaussian motions around the peptide axis is illustrated in **Figure S4**, which shows helical waves for tilt angles in the range of 0º-90º for distributions with σ_ρ = 0º, 10º, 20º, 50º or 100º. Note that the splittings are plotted as absolute values, since their sign is not revealed by ^{2}H-NMR experiments; however the averaging is calculated using signed splittings. Naturally, the shape of the curves is highly sensitive to the tilt angle. The curves are flat for τ = 0º; while for small tilt angles up to 30º they display two maxima. At higher tilt angles the waves become more complicated up to τ = 60º, when they develop four maxima as τ gets close to 90º. Additionally, with all the curves plotted on the same scale, it can be noted that also their amplitude changes with σ_ρ. The column of plots on the very left of **Figure S4** corresponds to peptides with a fixed rotational angle (σ_ρ = 0º). With increasing amplitude of the ρ-distribution (towards the right), the curves get more averaged and smeared out, until at very large values ($\sigma_\rho \rightarrow \infty$), all curves will completely average to a flat line. Such limiting case would correspond to fast rotation around the helical axis with equal probability for all ρ values, hence all labeled positions would then give the same splitting. Incomplete averaging gives some interesting results (7). For example, the shape of the curve for σ_ρ = 20º, τ = 45º is very similar to the shape for σ_ρ = 0º, τ = 40º, and the curve for σ_ρ = 50º, τ = 35º is almost identical to that for σ_ρ = 0º, τ = 20º (highlighted in **Figure S4**). Although the waves can still be distinguished by their amplitude, different alternatives may fit equally well to the data whenever a scaling factor is included in the analysis (see below).

It is also clear from **Figure S4** that for tilt angles close to 0º or 90º, the shape of the wave is not very sensitive to σ_ρ. In such cases, the tilt angle is well defined and can be reliably extracted from the rmsd fit. There are also some curves which are more unique; for example the wave corresponding to σ_ρ = 0º and τ = 65º does not seem to be reproducible by other combinations of σ_ρ and τ, and in this case it should be possible to have well-defined values of both the tilt angle and σ_ρ.

Influence of σ_τ on the helical wave plots

The general averaging effect due to a Gaussian distribution of tilt angles is illustrated in **Figure S5**, which shows helical waves for tilt angles in the range of 0º-90º for distributions with σ_τ = 0º, 10º, 20º, 50º or 100º. The small allowed σ_τ values for the transmembrane (small tilt) peptides can be understood from the effect of σ_τ on helical curves, since the shape of the waves for small tilt angles at σ_τ = 0º cannot be reproduced with larger values of this parameter. This is not the case for peptides with a tilt near 90º, for which similar wave shapes can be obtained both for a static molecule (σ_τ = 0º) and for one with significant wobbling (σ_τ up to 20º). For intermediate tilts and compared with the effect of σ_ρ, the general effect of σ_τ goes partly in the opposite direction. For example, the curves for σ_τ = 0º, τ = 35º; σ_τ = 10º, τ = 30º; and σ_τ = 20º, τ = 20º (highlighted in **Figure S5**), have similar shapes (except for the amplitudes). This means that when the peptide is mobile (with a wide τ distributions), a fit with the static model will underestimate the tilt angle. Additionally, while a large value of σ_ρ gives a flattened curve, a large value of σ_τ gives a shape similar to that of τ = 90º in a static peptide. However, such extreme values of σ_τ would correspond to peptides rotating almost freely around an axis perpendicular to the helix axis, which is unrealistic in the membrane environment.

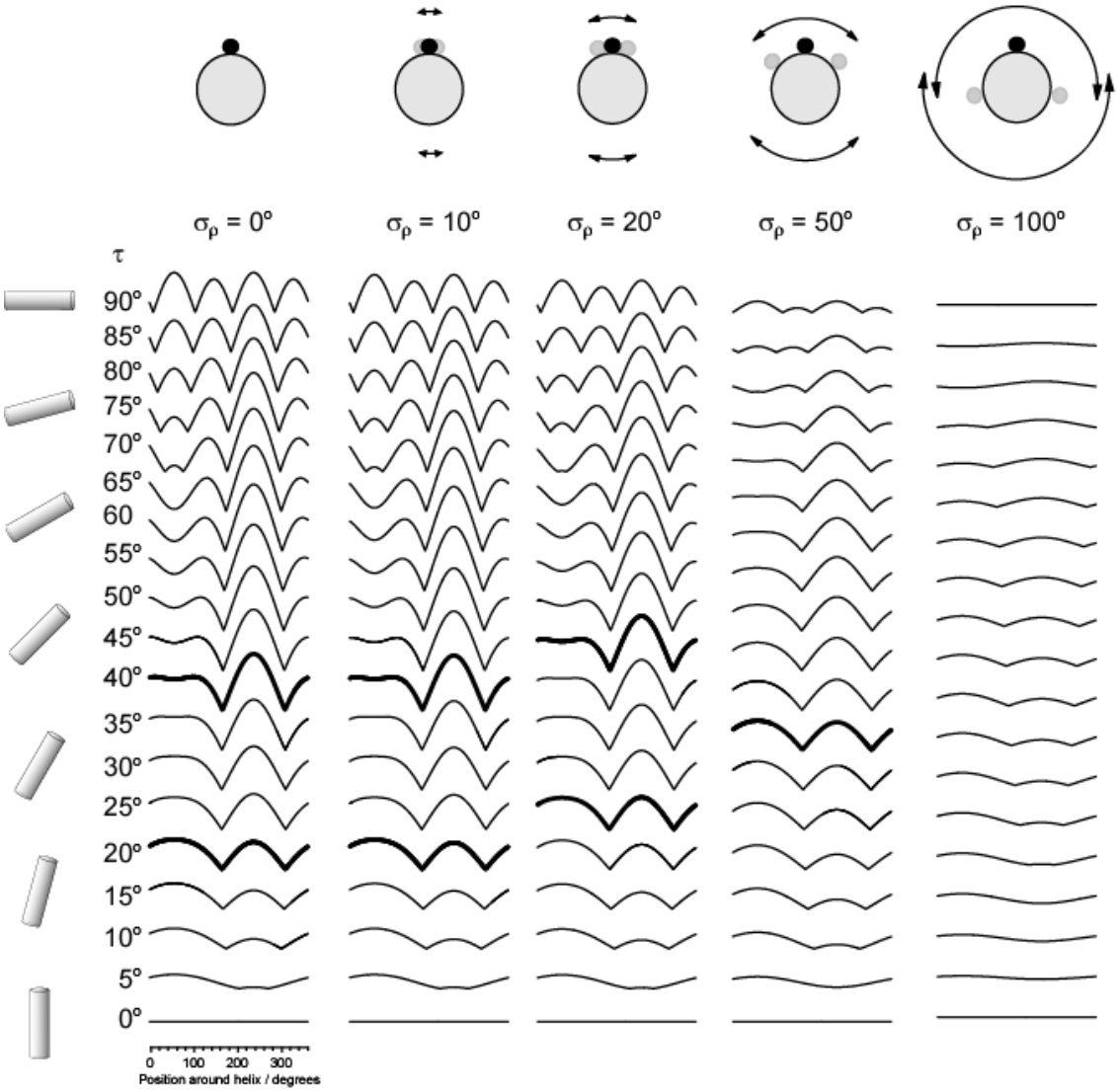

Figure S4. Quadrupolar helical waves for different τ angles (as indicated on the left) calculated with different distributions around ρ_0 (σ_ρ indicated above each column) as in Model 4. All curves are plotted on the same scale and show how the quadrupolar splittings vary around the helical axis. In all cases $\rho_0 = 0°$, and different values of ρ_0 would simply correspond to a horizontal shift of the curves. Some curves for different values of τ and σ_ρ but similar shapes are highlighted.

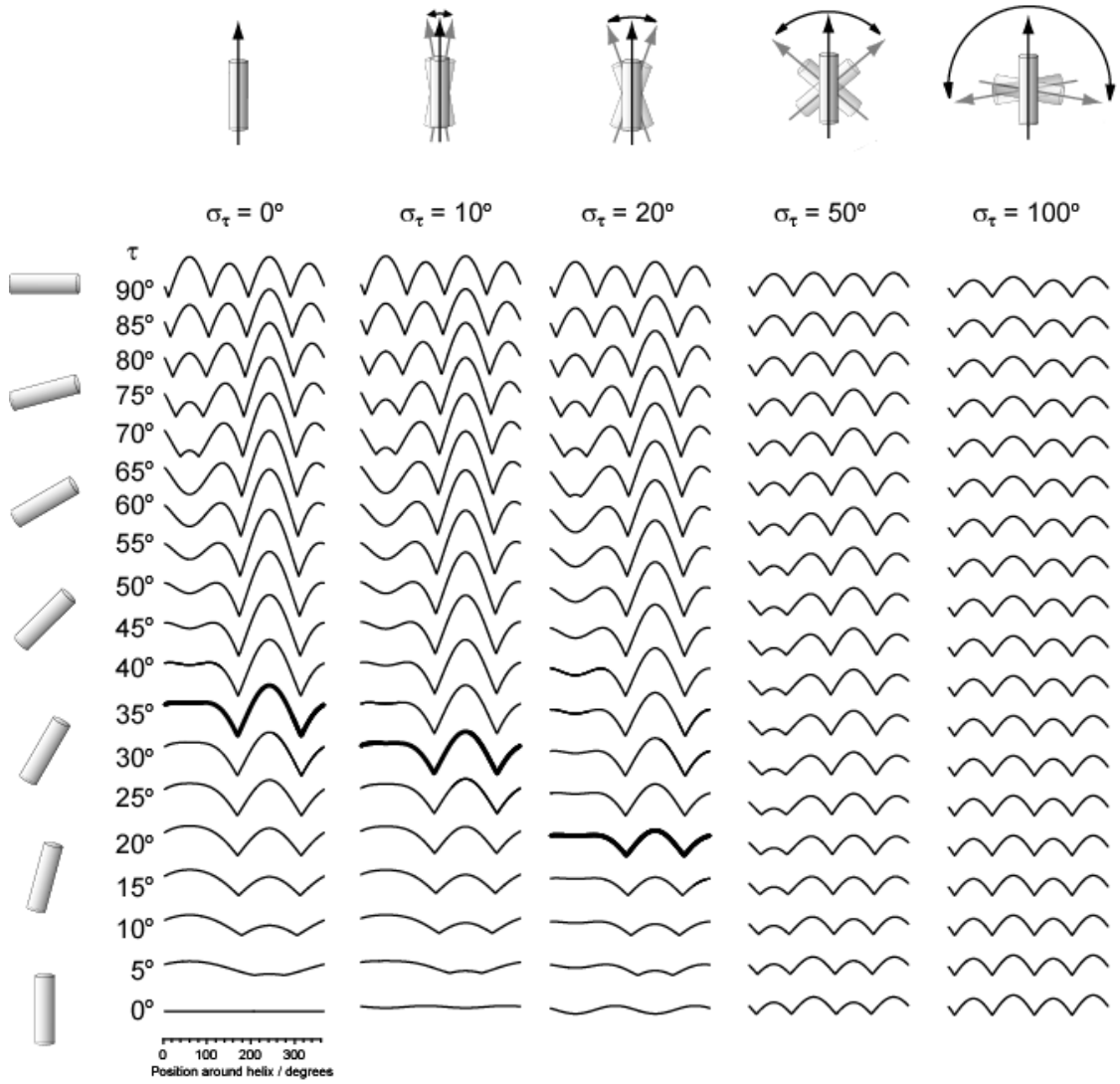

Figure S5. Quadrupolar helical waves for different τ angles (as indicated on the left) calculated with different distributions around τ_0 (σ_τ indicated above each column) as in Model 5. All curves are plotted on the same scale and show how the quadrupolar splittings vary around the helical axis. In all cases $\rho_0 = 0^o$, and different values of ρ_0 would simply correspond to a horizontal shift of the curves. Some curves for different values of τ and σ_τ but similar shapes are highlighted.

4. Detailed analysis of Model 5

For PGLa in the S-state, similar to the effect of the ρ distribution, there is a clear minimum in the rmsd curve as a function of σ_τ, with a best fit for $\sigma_\tau = 26^o$ (**Figure S6A**). Thus, it seems that Gaussian averaging of either the τ angle (Model 5) or the ρ angle (Model 4) has a similar ability to describe this system, with comparable quality of the fits (similar minimum rmsd). Additionally, τ increases slightly with increased σ_τ and ρ is virtually constant, so that also for this model, values of τ_0 and of ρ are well defined.

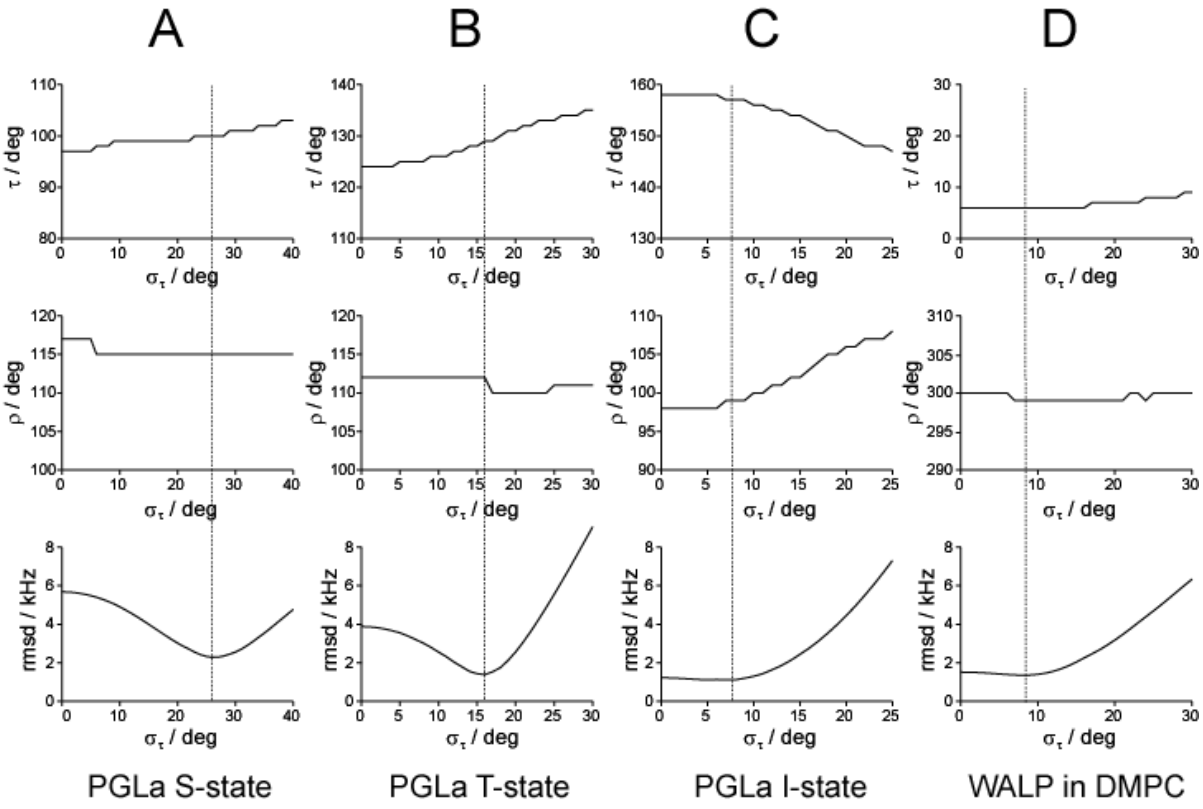

Figure S6. Finding the best-fit value for the fluctuations of the tilt angle σ_τ, and visualization of the corresponding variations in ρ and τ_0 (Model 5). The dashed line in each case indicates the best fit. (A) PGLa in the S-state, giving $\sigma_\tau = 26°$, $\tau_0 = 100°$. (B) PGLa in the T-state, giving $\sigma_\tau = 16°$, $\tau_0 = 129°$. (C) PGLa in the I-state, giving $\sigma_\tau = 8°$, $\tau_0 = 157°$. (D) WALP23 in DMPC, giving $\sigma_\tau = 8°$, $\tau_0 = 6°$. WALP23 in DLPC has a similar appearance as in DMPC (data not shown).

For PGLa in the T-state (**Figure S6B**), the curve has a similar appearance, but the best fit value of σ_τ is smaller, 16º, in the same range as σ_ρ. This decreased mobility compared to PGLa in the S-state (at a peptide-to-lipid ratio of 1:200) is in agreement with the proposed formation of dimers at this concentration (1:50). The tilt angle is sensitive to this kind of motion and increases with increased σ_τ value, but the best fit value of 129º is only 3º higher than for Model 3 with variable *S*, although with a slightly larger rmsd compared to this latter case (1.4 kHz *vs.* 1.2 kHz). For PGLa in the I-state (**Figure S6C**), there is a minimum rmsd value at σ_τ = 8º, but this is much more shallow than for PGLa in the S- or T-states. All σ_τ values from 0º to 10º give similar rmsd values close to 1.3 kHz, but for higher σ_τ values the rmsd increases steeply. τ_0 decreases slightly and ρ increases slightly with increased σ_τ, although both orientation angles appear to be reasonably well defined. In the case of WALP23 in DMPC there is a shallow rmsd minimum for σ_τ = 7º, but as for PGLa in the I-state it seems to be more appropriate giving an upper limit of σ_τ, in this case around 12º, where the rmsd curve starts rising (**Figure S6D**). Below this threshold σ_τ value, τ_0 is almost constant at ~5º, and changes in ρ are also small, so that values of τ_0 and ρ are well defined and do not depend much on σ_τ. However, the best fit rmsd (1.3 kHz) is considerably worse than for the ρ distribution Model 4 (see **Table 2** of the main text). For WALP in DLPC a similar behavior is obtained (result shown in **Table 2** but not in **Figure S6**).

5. Influence of S^i on the fits of Models 4, 5 and 6

Fit using S^i = 1

For the results described in **Table 2** in the main text, the fits were all performed using $\Delta\nu_q^0$ = 74 kHz (S^i=0.88). This takes into account intrinsic mobility of the peptide as seen in the ^{2}H-NMR splittings for peptides in a dry powder. Amphipathic peptides such as PGLa often have no defined structure in solution, and thus also not in powder, and only form an α-helix in the presence of a membrane. It is therefore not meaningful to attribute the mobility in a powder to rotation of and around a peptide helix axis in this case. If it is assumed that the dynamics of the peptide can be described exclusively using σ_ρ and σ_τ, then the fit should be performed using $\Delta\nu_q^0$ = 84 kHz (S^i=1.00). The results for the studied peptide systems for Models 3, 4 and 5 in this case are presented in **Tables S1** and **S2**.

Assuming that there is no intrinsic motion of the peptides (S^i=1), the explicit dynamic models give, as could be expected, wider distributions of angles. The increase in σ_ρ and σ_ρ compared to using S^i=0.88 is about 5º. No significant change in the orientation is found. The rmsd is somewhat higher for Model 4 and Model 5, but is identical for Model 6, for both values of S^i. The exact amount of intrinsic motion is somewhat uncertain, but do not influence the result much, and it is possible to get rather good estimates of the dynamics using Model 6.

Table S1. Best fit parameters using Gaussian distributions of either ρ (Model 4) or τ (Model 5), in both cases with $\Delta\nu_q^0$ = 84 kHz (S^i=1.00).

Peptide/lipid system	Model 4				Model 5			
	τ / º	ρ_0 / º	σ_ρ / º	rmsd/ kHz	τ_0 / º	σ_τ / º	ρ / º	rmsd /kHz
PGLa in the S-state*	95	117	25	2.3	102	34	115	2.8
PGLa in the T-state*	119	110	27	1.8	132	22	111	1.7
PGLa in the I-state†	146-161	94-97	1-52	2.3-2.4	159	13	101	1.5
WALP23 in DMPC‡	23	305 (155)	106	0.9	5	8	298 (162)	2.0
WALP23 in DLPC‡	37	317 (143)	99	2.3	7	16	288 (172)	3.2

* From (3)
† From (5)
‡ From (6). The ρ values calculated according to the conventions of the original WALP23 publication are given in brackets to allow comparison with the previous analysis.

Table S2. Best fit parameters using the distributions of both τ and ρ angles (Model 6), with $\Delta\nu_q^0$ = 84 kHz (S^i=1.00).

Peptide/lipid system	τ_0 / º	σ_τ / º	ρ_0 / º	σ_ρ / º	rmsd/kHz
PGLa in the S-state*	98	21	115	19	2.0
PGLa in the T-state*	124	16	111	21	1.2
PGLa in the I-state†	153	15	98	31	1.1
WALP23 in DMPC‡	15	21	302 (158)	74	0.9
WALP23 in DLPC‡	31	30	317 (143)	68	2.2

* From (3)
† From (5)

‡ From (6). The ρ values calculated according to the conventions of the original WALP23 publication are given in brackets to allow comparison with the previous analysis.

Fit combining *S*, σ_ρ and σ_τ

It might be argued that a scaling factor *S* should be used to account for additional motions apart from those represented by the τ and ρ fluctuations. However, the non-specific averaging effect of *S* on the ^{2}H splittings overlaps with the effect of the ρ- and τ-distributions and would make the system more ambiguous. For instance, when the ρ distribution model is used in combination with a variable scaling factor, it is not possible to find a unique minimum rmsd, but instead multiple solutions are found for any value of σ_ρ from zero to some upper limit, each one with a different combination of the *S* value and different tilt and azimuthal angles (data not shown). Something similar happens if we combine a variable *S* with a distribution of τ, or with distributions of both τ and ρ. Thus, unless σ_ρ and σ_τ are known from an independent method, it is not possible to extract a value of *S* corresponding to other types of motion. Alternatively, to describe the whole-body wobbling of a rigid rod-like α-helix, one could deconvolute the ^{2}H-NMR data in terms of a complete order parameter tensor, which would also require an rmsd fit of 5 free parameters. From a mathematical point of view this approach is the only valid treatment, but one would still face the difficulty of interpreting the order parameter tensor in terms of a motional model.

References

1. Glaser, R. W., C. Sachse, U. H. N. Dürr, S. Afonin, P. Wadhwani, E. Strandberg, and A. S. Ulrich. 2005. Concentration-dependent realignment of the antimicrobial peptide PGLa in lipid membranes observed by solid-state ^{19}F-NMR. *Biophys. J.* 88:3392-3397.
2. Glaser, R. W., C. Sachse, U. H. Dürr, P. Wadhwani, and A. S. Ulrich. 2004. Orientation of the antimicrobial peptide PGLa in lipid membranes determined from ^{19}F-NMR dipolar couplings of 4-CF_3-phenylglycine labels. *J. Magn. Reson.* 168:153-163.
3. Strandberg, E., P. Wadhwani, P. Tremouilhac, U. H. N. Dürr, and A. S. Ulrich. 2006. Solid-state NMR analysis of the PGLa peptide orientation in DMPC bilayers: structural fidelity of ^{2}H-labels versus high sensitivity of ^{19}F-NMR. *Biophys. J.* 90:1676-1686.
4. Tremouilhac, P., E. Strandberg, P. Wadhwani, and A. S. Ulrich. 2006. Conditions affecting the re-alignment of the antimicrobial peptide PGLa in membranes as monitored by solid state ^{2}H-NMR. *Biochim. Biophys. Acta* 1758:1330-1342.
5. Tremouilhac, P., E. Strandberg, P. Wadhwani, and A. S. Ulrich. 2006. Synergistic transmembrane alignment of the antimicrobial heterodimer PGLa/magainin. *J. Biol. Chem.* 281:32089-32094.
6. Strandberg, E., S. Özdirekcan, D. T. S. Rijkers, P. C. A. Van der Wel, R. E. Koeppe, II, R. M. J. Liskamp, and J. A. Killian. 2004. Tilt angles of transmembrane model peptides in oriented and non-oriented lipid bilayers as determined by ^{2}H solid state NMR. *Biophys. J.* 86:3709-3721.
7. Esteban-Martin, S. and J. Salgado. 2007. The dynamic orientation of membrane-bound peptides: bridging simulations and experiments. *Biophys. J.* 93:4278-4288.